Final Report

# Scientific Study in Solar and Plasma Physics Relative to Rocket and Balloon Projects

NAS8-38609 DO 20

Period of Performacne: December 9, 1993 - December 8, 1993

Prepared by:

Dr. S. T.Wu
Department of Mechanical and Aerospace Engineering
and Center for Space Plasma and Aeronomic Research
The University of Alabama in Huntsville
Huntsville, AL 35899

(NASA-CR-193885) SCIENTIFIC STUDY IN SOLAR AND PLASMA PHYSICS RELATIVE TO ROCKET AND BALLOON PROJECTS Final Report, 9 Dec. 1991 - 8 Dec. 1993 (Alabama Univ.) 31 p

N94-24461

Unclas

G3/92 0204202

NASA
National Aeronautics and Space Agency

# Report Document Page

| 1. Report No. | 2. Government Accession No. | 3. Recipient's Catalog No. |
|---|---|---|
| Final | | |

| 4. Title and Subtitle | 5. Report Due |
|---|---|
| Scientific Study in Solar and Plasma Physics Relative to Rocket and Balloon Projects | 11/93 |
| | 6. Performing Organization Code: University of Alabama in Huntsville |
| 7. Aurthor(s) | 8. Performing Organization Report No. |
| S. T. Wu | Final |
| | 10. Work Unit No. |
| 9. Performing Organization Name and Address | 11. Contract or Grant No. |
| University of Alabama in Huntsville<br>Huntsville, Alabama 35899 | NAS8-38609 DO 20 |
| 12. Sponsoring Agency Name and Address | 13. Type of report and Period covered |
| National Aeronautics and Space Administration<br>Washington, D.C. 20546-001<br>Marshall Space Flight Center, AL 35812 | Draft Final 12/9/91 - 12/8/93 |
| | 14. Sponsoring Agency Code |

15. Supplementary Notes

16.Abstract


Provide scinetific and technical capabilities in areas of solar and plasma physics contained in research programs and instrumentation development relative to current rocket and ballon projects.

Develop flight instrumentation design, flight hardware, and flight program objectives and participate in peer reviews as appropriate.

Participate in solar-terrestrial physics modeling studies and analysis of flight data and provide theoretical investigations as required by these studies.


| 17. Key Words (Suggested by Author(s)) | 18. Distribution Statement |
|---|---|
| Solar Physics<br>Plasma Physics | CN22D,3; AT01,1; Em13/L.Smith,1;<br>ONRRR,1; ES-52/Reichman,1+repro;<br>NASA/Sci&TEch Info Fac.,1+repro;<br>Vaughn/UAH,1. |

| 19. Security Class. (of this report) | 20. Security Class. (of this page) | 21. No. of pages | 22. Price |
|---|---|---|---|
| Unclassified | Unclassified | 32 | - |

NASA FORM 1626 OCT 86

In April of 1992 Dr. Robert Stein visited Dr. D. Hathaway (SSL/MSFC/NASA) and the P.I. to discuss magnetohydrodynamic waves through the solar atmosphere.

Dr. Marta Rovira, from the Institute of Astronomy at Buenos Aires, Argentina visited SSL/MSFC/NASA and the University for a two week period in April 1992 to discuss solar physics and magnetic field research.

September 1992 the P.I. had extensive discussions with the SSL/MSFC/NASA personnel (Dr. J. Davis) concerning the plans for the instrumentation development on board rocket projects. In particular the development of vector solar magnetograph on balloon flights.

Dr. Robert Rosner was invited and accepted an invitation to returned to Huntsville in March 1993 to discuss further the present magnetohydrodynamic wave generation on the solar surface and its effects on the dynamics in the solar and stellar atmosphere.

Dr. S. T. Wu and Dr. J. Davis again discussed the development of vector solar magnetograph on balloon flights as part of the instrumentation planning of rocket projects in June 1993.

In October 1993 Dr. Chin-Chun Wu performed asstudy of slow shock evoluiton by numerical simulation modeling and gave a report to the P.I. These results are scheduled to be presented at the 1993 Annual Fall Meeting of the Amerian Geophysical Union. Some of the key results are included in the appendix.

# APPENDIX

**Numerical Study on the MHD Slow Shock Generation and Propagation in the Solar Wind**

S. T. Wu, C. C. Wu, (Center for Space Plasma and Aeronomic Research and Department of Mechanical Engineering, The University of Alabama in Huntsville, Huntsville, AL 35899; 205-895-6413; e- mail wu@cspara.dnet.nasa.gov)
S. T. Suess, Space Science Laboratory, NASA/MSFC, Huntsville, AL 35812
J. K. Chao, Institute of Space Science, National Central University, Chung li, Taiwan, Republic of China

It is well-known that most MHD shocks observed at 1 AU are MHD fast shocks. Only very limited number of MHD slow shocks are observed at 1 AU. In order to understand why there are only a few MHD shocks observed at 1 AU we have performed a numerical study using an adaptive grid, unsteady, two-dimensional MHD model (Pantichob, Wu and Suess, 1987 AIAA Paper 87-1218, Washington, DC) to investigate the MHD slow shock generation and propagation in the solar wind. In these numerical experiments a total of twenty-two cases of numerical calculations with various boundary perturbation are performed. These numerical results are summarized as follows:

1. The forward slow shock (FSS) and reversed slow shock (RSS) can pass through each other and keep its own characteristics
2. The second FSS will catch the first FSS and emerge into a stronger FSS.
3. The FSS always disappears within a distance of 140 $R_S$ (solar radii) from the sun when there is a forward fast shock propagating in front of them.
4. When a FSS propagates behind a FFS, it shows the decreasing mach number of FSS.
5. When a FSS propagates in front of a forward fast shock (FFS), it always will be caught by the FFS and destroyed by it.
6. In all the tests we hve performed we have not discovered that the FSS (RSS) evolves into a FFS.

This work supported by NASA Headquarters Grant NAGW-9.

1. 1993 Fall Meeting
2. 000610709
3. (a) S. T. Wu
   M&A Engr., UAH
   HSV, AL 35899
   (b) Tel: 205-895-6413
   (c) Fax: 205-895-6382
4. SPA
5. SHO3
6. Poster
7. 0%
8. $50 check enclosed
9. C
10. n/a
11. No

# NUMERICAL STUDY ON THE MHD SLOW SHOCK GENERATION AND PROPAGATION IN THE SOLAR WIND

**S. T. Wu, C. C. Wu*** (Center for Space Plasma and Aeronomic Research and Department of Mechancial and Aerospace Engineering, The University of Alabama in Huntsville, Huntsville, AL 35899 USA
**S. T. Suess**, Space Science Laboratory, National Aeronautics and Space Administration/George C. Marshall Space Flight Center (NASA/MSFC), Marshall Space Flight Center, AL 35899 USA
and **J. K. Chao**, Institute of Space Science, National Centeral University, Chung li, Taiwan, ROC

*Also Institute of Space Science, National Centeral University, Chung li, Taiwan, ROC

## OBJECTIVES

It is well-known that most MHD shocks observed at 1 AU are MHD fast shocks. Only very limited number of MHD slow shocks are observed at 1 AU. In order to understand why there are only a few MHD slow shocks observed at 1 AU we have performed a numerical study using an adaptive grid, unsteady, two-dimensional MHD model (Pantichob, Wu and Suess, 1987 AIAA Paper 87-1218, Washington, DC) to investigate the MHD slow shock generation and propagation in the solar wind.

## NUMERICAL MODEL

This study is based on a numerical model entitled "An Adaptive Grid, Unsteady Model for a Two-Dimensional MHD Flow" given by Panitchob, Wu and Suess (1987). Since this model has only adaptive grid along the radial direction, we surpress this code to one-dimension (radial flow) for this study. The steady-state is the typical quiet solar wind solution:

**TABLE I. Summary of Steady State Values at 28 $R_s$ and 1 AU**

| Dependent Variable | Steady State Value at 28 $R_s$ | Steady State Value at 1 AU |
|---|---|---|
| T, K | $3.7684 \times 10^5$ | $1.3 \times 10^5$ |
| $\rho$, gm/cm$^3$ | $1.026 \times 10^{-21}$ | $1.453 \times 10^{-23}$ |
| $V_r$, km/s | 261.28 | 312.890 |
| $V_\phi$, km/s | 4.0012 | 1.263 |
| $B_r$, gauss | $2.948 \times 10^{-3}$ | $5 \times 10^{-5}$ |
| $B_\phi$, gauss | $-6.1357 \times 10^{-4}$ | $-7.143 \times 10^{-5}$ |
| $\gamma$: Polytrophic Index | 1.25 | 1.25 |

## NUMERICAL EXPERIMENTS FOR SIMULATION OF SHOCKS (0NE-DIMENSIONAL STUDY)

In the present formulation, there are six parameters (i.e. $\rho$, T, $V_r$, $V_\phi$, $B_r$, and $B_\phi$) which can be perturbed to generate MHD shocks. Since $\nabla \cdot \vec{B} = 0$ must be satisfied, it implies that $r^2 B_r$ = constant for the one-dimension case. In addition, the $\phi$-components of velocity and magnetic field are two orders of magnitude smaller than the r-components. Thus we simply ignore the effects of the $\phi$-components perturbations. Therefore, we shall focus our study on the perturbation of the physical parameters, $\rho$, $V_r$, and T. On the basis if this scenario, we classify the perturbation into the following six catagories as shown in Figure 1. Using these forms of perturbations with various combinations of physical parameters ($\rho'/\rho_0$, $v'/v_0$, $T'/T_0$), we have performed 22 experiments. These 22 experiments are depicted in Table II.

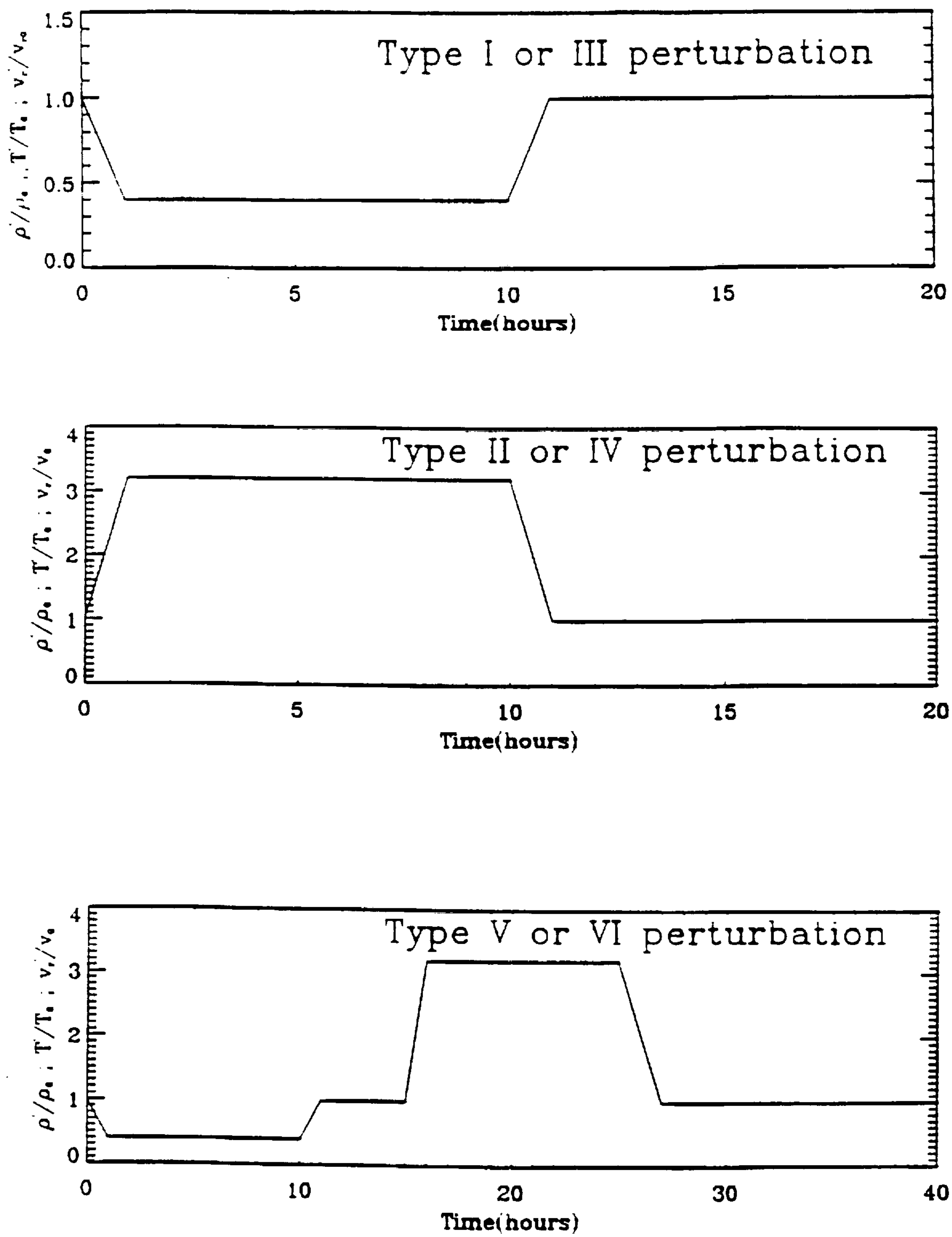


Figure 1. The Types of Perturbations.

Table II Listing of 22 Cases of Six Different Types of Perturbations

| | first perturbation | | | second perturbation | | | |
|---|---|---|---|---|---|---|---|
| Case | $\frac{\rho'}{\rho_o}$ | $\frac{v_r'}{v_{r_o}}$ | $\frac{T'}{T_o}$ | $\frac{\rho''}{\rho_o}$ | $\frac{v_r''}{v_{r_o}}$ | $\frac{T''}{T_o}$ | Perturbation Type |
| 1 | 0.4 | | | | | | I |
| 2 | 0.8 | | | | | | I |
| 3 | | 0.4 | | | | | I |
| 4 | | 0.8 | | | | | I |
| 5 | | | 0.4 | | | | I |
| 6 | | | 0.8 | | | | I |
| 7 | 1.6 | | | | | | II |
| 8 | 3.2 | | | | | | II |
| 9 | | 1.6 | | | | | II |
| 10 | | 2.0 | | | | | II |
| 11 | | | 1.6 | | | | II |
| 12 | | | 3.2 | | | | II |
| 13 | 0.4 | 0.4 | | | | | III |
| 14 | 0.4 | | 0.4 | | | | III |
| 15 | | 0.4 | 0.4 | | | | III |
| 16 | 5.0 | 1.6 | | | | | IV |
| 17 | 2.0 | | 5.0 | | | | IV |
| 18 | | 1.6 | 5.0 | | | | IV |
| 19 | | | 0.4 | | | 3.2 | V |
| 20 | 0.4 | 0.4 | | 5.0 | 1.6 | | VI |
| 21 | | 0.4 | 0.4 | 5.0 | 1.6 | | VI |
| 22 | | 0.4 | 0.4 | | 1.6 | 5.0 | VI |

where subscript "o" denotes the initial values at the reference point, which is at 28 $R_S$; superscript "′" denotes the variable value of first perturbation; "″" denotes the variable value of second perturbation at the low boundary which is at 28 $R_S$ for this study; 0.4 (0.8) means the perturbation decreasing to 40 percent (80 percent) of its initial value; 1.6 (2.0, 3.2, 5.0) denotes the variable of the perturbation increasing to 160 (200, 320, 500) percent of its initial value.

# NUMERICAL RESULTS

In this presentation we only show the representative cases.

**I. Single Pulse (i.e. square wave) Perturbation**

The perturbations of Type I, II, III, and IV belong in this category. Their characteristics are summarized in Tables III, IV, V, and VI, respectively. From these results we found:

1. From the numerical results of Type I and III, we notice the following:
   (a) the negative square wave perturbation generated a pair of slow shocks (one FSS and one RSS). The shock strength of these SSs increases as they propagate toward Earth. (see Tables III and IV).
   (b) when the RSS and FSS cross each other their characteristics are preserved. (see Figure 2).
   (c) Once the FSS is formed, it will propagate toward Earth without evolving to a FFS.
2. From the simulation of Type II and IV perturbations, we note the following:
   (a) The positive square wave disturbance gives birth to both slow shocks (SS) and fast shocks (FS), it shows that FFS takes longer time to develop in comparison to FSS (see Figure 3).
   (b) The strength of the FFS increases with radial distance but the strength of the FSS behaves opposite. (see Tables IV and Figure 3).
   (c) The FSS with a mach number $< 2.5$ propagates behind a FFS with a mach number $> 1.7$, this FSS will disappear near 140 $R_S$.

## Table III. Summary Results of Type I Perturbations

| case | perturbation | FSS | | | | |
|---|---|---|---|---|---|---|
| | | formed Time (hrs) | formed r ($R_s$) | ave. $M_s$ | $M_s$ at 35 $R_s$ | $M_s$ at 200 $R_s$ |
| 1 | $\frac{\rho'}{\rho_o} = 0.4$ | 11 | 29.8 | 1.68 | 1.41 | 1.87 |
| 2 | $\frac{\rho'}{\rho_o} = 0.8$ | 13 | 33.5 | 1.42 | 1.21 | 1.62 |
| 3 | $\frac{v'_r}{v_{r_o}} = 0.4$ | 13 | 31.7 | 2.33 | 2.08 | 2.41 |
| 4 | $\frac{v'_r}{v_{r_o}} = 0.8$ | 13 | 32.1 | 1.70 | 1.68 | 1.95 |
| 5 | $\frac{T'}{T_o} = 0.4$ | 13 | 33.1 | 1.72 | 1.15 | 2.27 |
| 6 | $\frac{T'}{T_o} = 0.8$ | 13 | 33.1 | 1.47 | 1.63 | 1.66 |

| case | perturbation | RSS | | | | |
|---|---|---|---|---|---|---|
| | | formed Time (hrs) | formed r ($R_s$) | ave. $M_s$ | $M_s$ at 35 $R_s$ | $M_s$ at 150 $R_s$ |
| 1 | $\frac{\rho'}{\rho_o} = 0.4$ | 3 | 29.5 | 1.78 | 1.77 | 2.31 |
| 2 | $\frac{\rho'}{\rho_o} = 0.8$ | 3 | 29.6 | 1.54 | 1.50 | 1.64 |
| 3 | $\frac{v'_r}{v_{r_o}} = 0.4$ | 13 | 29.4 | 1.86 | 1.95 | 1.83 |
| 4 | $\frac{v'_r}{v_{r_o}} = 0.8$ | 13 | 29.6 | 1.54 | 1.68 | 1.95 |
| 5 | $\frac{T'}{T_o} = 0.4$ | 3 | 29.9 | 1.76 | 1.70 | 2.00 |
| 6 | $\frac{T'}{T_o} = 0.8$ | 3 | 29.7 | 1.55 | 1.51 | 1.73 |

Table IV. Summary Results of Type II Perturbations

| | | FFS | | | | |
|---|---|---|---|---|---|---|
| | | formed | | | $M_f$ at | |
| case | perturbation | Time (hrs) | r ($R_s$) | ave. $M_f$ | 100 $R_s$ | 200 $R_s$ |
| 7 | $\frac{v_r'}{v_{r_0}} = 1.6$ | 9 | 50.0 | 1.38 | 1.33 | 1.70 |
| 8 | $\frac{v_r'}{v_{r_0}} = 2.0$ | 7 | 45.9 | 1.76 | 1.78 | 2.09 |
| 9 | $\frac{\rho'}{\rho_0} = 1.6$ | 33 | 94.3 | 1.08 | 1.04 | 1.12 |
| 10 | $\frac{\rho'}{\rho_0} = 3.2$ | 19 | 69.9 | 1.12 | 1.05 | 1.22 |
| 11 | $\frac{T'}{T_0} = 1.6$ | 19 | 66.8 | 1.07 | 1.04 | 1.13 |
| 12 | $\frac{T'}{T_0} = 3.2$ | 21 | 75.4 | 1.30 | 1.12 | 1.55 |
| | | FSS | | | | |
| | | formed | | | $M_s$ at | |
| case | perturbation | Time (hrs) | r ($R_s$) | ave. $M_s$ | 60 $R_s$ | 200 $R_s$ |
| 7 | $\frac{v_r'}{v_{r_0}} = 1.6$ | 3 | 33.2 | 1.83 | 2.00 | 1.42 |
| 8 | $\frac{v_r'}{v_{r_0}} = 2.0$ | 3 | 33.6 | 2.01 | 2.40 | 1.48 |
| 9 | $\frac{\rho'}{\rho_0} = 1.6$ | 15 | 54.4 | 1.51 | 1.50 | 1.42 |
| 10 | $\frac{\rho'}{\rho_0} = 3.2$ | 5 | 37.1 | 1.66 | 1.78 | 1.66 |
| 11 | $\frac{T'}{T_0} = 1.6$ | 9 | 44.0 | 1.50 | 1.52 | 1.47 |
| 12 | $\frac{T'}{T_0} = 3.2$ | 5 | 37.1 | 1.79 | 1.89 | 1.47 |
| | | RSS | | | | |
| | | formed | | | $M_s$ at | |
| case | perturbation | Time (hrs) | r ($R_s$) | ave. $M_s$ | 35 $R_s$ | 150 $R_s$ |
| 7 | $\frac{v_r'}{v_{r_0}} = 1.6$ | 3 | 31.3 | 2.28 | 2.11 | 2.64 |
| 8 | $\frac{v_r'}{v_{r_0}} = 2.0$ | 3 | 32.2 | 2.82 | 2.54 | 2.56 |
| 9 | $\frac{\rho'}{\rho_0} = 1.6$ | 13 | 29.6 | 1.61 | 1.49 | 1.77 |
| 10 | $\frac{\rho'}{\rho_0} = 3.2$ | 13 | 29.6 | 1.79 | 1.76 | 1.78 |
| 11 | $\frac{T'}{T_0} = 1.6$ | 13 | 29.5 | 1.58 | 1.50 | 1.62 |
| 12 | $\frac{T'}{T_0} = 3.2$ | 3 | 29.7 | 1.55 | 1.12 | 1.55 |

Table V. Summary Results of Type III Perturbations

| Case | perturbation | FSS | | | | |
|---|---|---|---|---|---|---|
| | | formed Time (hrs) | formed r ($R_s$) | ave. $M_s$ | $M_s$ at 35 $R_s$ | $M_s$ at 200 $R_s$ |
| 13 | $\frac{v_r'}{v_{r_0}} = 0.4, \frac{T'}{T_0} = 0.4$ | 13 | 31.1 | 2.71 | 1.44 | 2.90 |
| 14 | $\frac{v_r'}{v_{r_0}} = 0.4, \frac{\rho'}{\rho_0} = 0.4;$ | 13 | 31.9 | 2.58 | 2.23 | 2.79 |
| 15 | $\frac{\rho'}{\rho_0} = 0.4, \frac{T'}{T_0} = 0.4;$ | 11 | 29.6 | 2.00 | 1.56 | 2.02 |

| Case | perturbation | RSS | | | | |
|---|---|---|---|---|---|---|
| | | formed Time (hrs) | formed r ($R_s$) | ave. $M_s$ | $M_s$ at 35 $R_s$ | $M_s$ at 150 $R_s$ |
| 13 | $\frac{v_r'}{v_{r_0}} = 0.4, \frac{T'}{T_0} = 0.4$ | 13 | 29.4 | 1.92 | 2.05 | 1.83 |
| 14 | $\frac{v_r'}{v_{r_0}} = 0.4, \frac{\rho'}{\rho_0} = 0.4;$ | 13 | 29.5 | 1.70 | 1.79 | 1.81 |
| 15 | $\frac{\rho'}{\rho_0} = 0.4, \frac{T'}{T_0} = 0.4;$ | 3 | 29.9 | 2.06 | 2.34 | 2.50 |

Table VI. Summary Results of Type IV Perturbations

| | | FFS | | | | |
|---|---|---|---|---|---|---|
| Case | perturbation | formed Time (hrs) | formed r ($R_s$) | ave. $M_f$ | $M_f$ at 60 $R_s$ | $M_f$ at 200 $R_s$ |
| 16 | $\frac{v_r'}{v_{r_0}} = 1.6, \frac{T'}{T_0} = 5.0$ | 5 | 40.1 | 1.79 | 1.35 | 2.14 |
| 17 | $\frac{\rho'}{\rho_0} = 5.0, \frac{v_r'}{v_{r_0}} = 1.6$ | 5 | 40.2 | 1.68 | 1.27 | 2.05 |
| 18 | $\frac{\rho'}{\rho_0} = 2.0, \frac{T'}{T_0} = 5.0$ | 11 | 54.0 | 1.71 | 1.16 | 2.04 |
| | | FSS | | | | |
| Case | perturbation | formed Time (hrs) | formed r ($R_s$) | ave. $M_s$ | disappear Time (hrs) | disappear r ($R_s$) |
| 16 | $\frac{v_r'}{v_{r_0}} = 1.6, \frac{T'}{T_0} = 5.0$ | 5 | 38.6 | 2.34 | 53 | 152.2 |
| 17 | $\frac{\rho'}{\rho_0} = 5.0, \frac{v_r'}{v_{r_0}} = 1.6$ | 5 | 38.3 | 2.39 | 45 | 131.1 |
| 18 | $\frac{\rho'}{\rho_0} = 2.0, \frac{T'}{T_0} = 5.0$ | 5 | 38.1 | 2.42 | 53 | 148.2 |

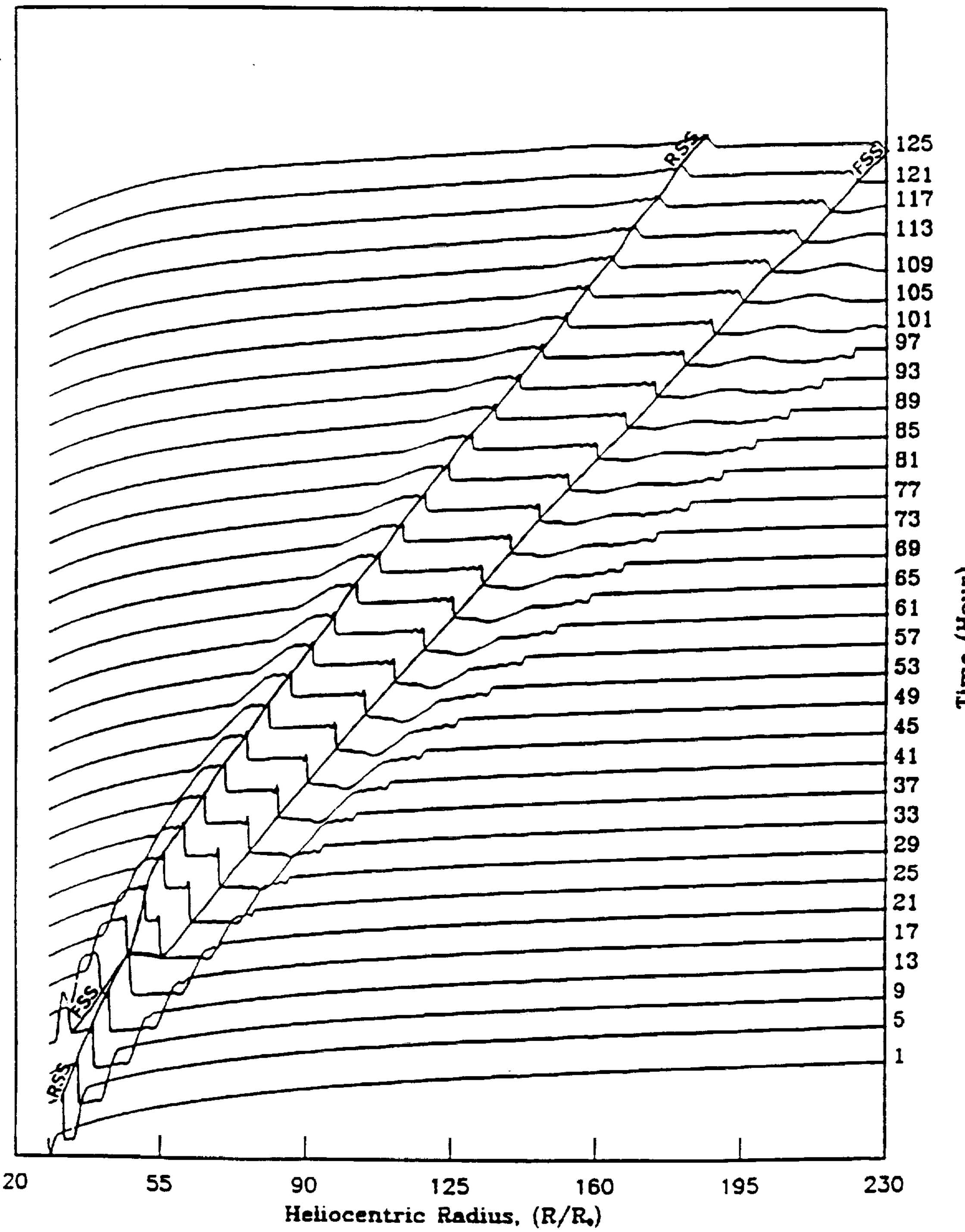


Figure 2. The evolution of radial velocity for case 1, $\frac{\rho'}{\rho_o} = 0.4$

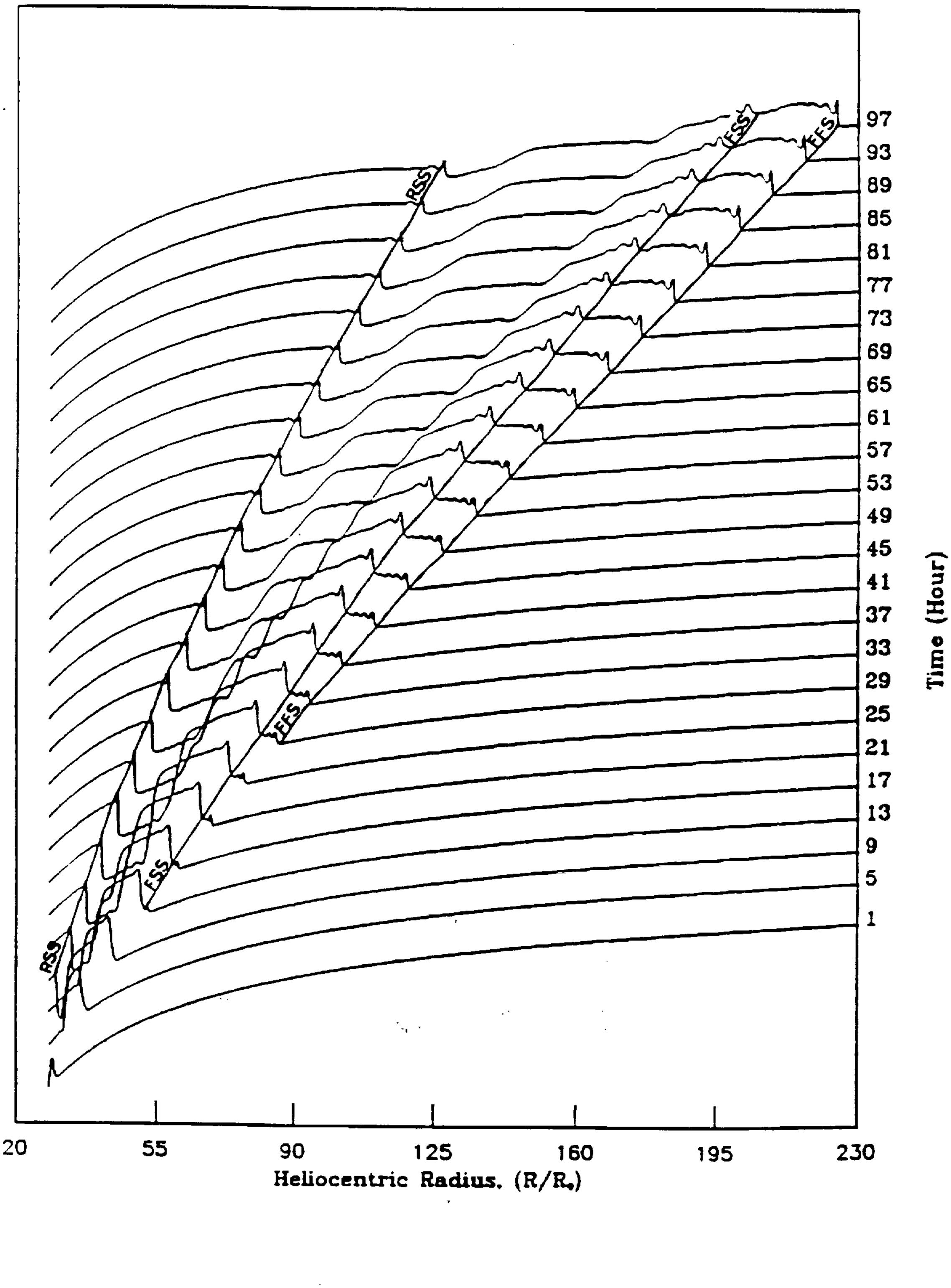


Figure 3. The evolution of radial velocity for case 9, $\frac{\rho'}{\rho_o} = 1.6$

## II. Multiple Pulses (Square Waves) Perturbations (i.e. Type V and VI): Shock -Shock Interactions

In this section we present the interactions between fast shocks (FS) and slow shocks (SS). To achieve these numerical experiments we combined the Type I and Type II perturbations which is named as Type V perturbation. A summary of numerical results is shown in Table VII and their radial velocity evolution is shown in Figure 4, 5, and 6. The numerical results due to Type VI are shown in Table VIIIa,b and their radial velocity evolution is shown in Figure 7 and 8. Note, the differences between Type V and Type VI perturbations are the perturbed physical parameters. From these results, we learned the following:

1. Case 19 shows that the second perturbation generated shocks (i.e. FSS(A) and RSS(A) will interact with the first perturbtion generated shocks (i.e. FFW(B), FFS(B) and FSS(B)). As shown in Figure 9, there are four waves (i.e. RSS(A), FSS(A), FFW(B) and FSS(B)) generated at t =2l hrs; the RSS(A) is in front of FSS(A); FFW(B) is behind FSS(A) and FFW(B) is followed by FSS(B). At t = 49 hrs, FFW(B) steepened into a FFS(B) after it caught the FFS(A) and RSS(B) from behind (see Figure 10). It showed that the FSS(A) and RSS(A) disappeared and the FSS(a) merged with FSS(B) into a stronger FSS(A+B).

2. Case 19b shows that the FFS(B) caught FSS(A) from behind, and the FSS(A) was destroyed by FFS(B). (see Figure 5).

3. The results of Case 19c are identical to Case 5 before we introduced the second perturbation into the system which has a FSS(A) and a RSS(A) at ~65 $R_S$. At t = 45 hrs (i.e. 20 hrs after we introduced the second perturbation) we observed a FFW(B) forming and followed by a FSS(B). In the meantime, the FSS(A) and RSS(A) were ahead of FFW(B). These four wave interactions are shown in Figure 6.

4. To illustrate the numerical results from Type VI perturbation we present Case 21a as shown in Table VIIIa and Figure 8. In this case, the second perturbation was introduced at t = 33 hrs, the results showed that a FSS(A) was fromed at 31.9 $R_S$ (t = 13 hrs), and the average shock strength was 2.58 (mach no.) before it was caught by the FFS(B) from behind. The FSS(A) disappeared at ~187 $R_S$ (t = 101 hrs). The FFS(B) was formed at ~66 $R_S$ (t = 49 hrs) and the shock strength is 1.83 (mach no.) The FSS(B) was formed at 36 $R_S$ (t = 37 hrs) and disappeared at 117 $R_S$ t = 73 hrs). At t = 69 hrs, we observed the FSS(A) in front of the FFS(B) and the FSS(B) behind the FFS(B). But at t = 73 hrs the FSS(B) disappeared and FSS(A) was caught by the FFS(B) from behind and destroyed FSS(A).

Table VII: Summary Results of Type V Perturbations

| | | FFS(B) | | | | | |
|---|---|---|---|---|---|---|---|
| Case | perturbation | formed at Time (hrs) | formed at r ($R_\circ$) | ave. $M_f$ | $M_s$ at 140 $R_\circ$ | $M_s$ at 180 $R_\circ$ | second perturbation starts at(hrs) |
| 19.a | $\frac{T'}{T_\circ} = 0.4; \frac{T''}{T_\circ} = 3.2$ | 49 | 100.0 | 1.36 | 1.41 | 1.55 | 15 |
| 19.b | $\frac{T'}{T_\circ} = 0.4; \frac{T''}{T_\circ} = 3.2$ | 69 | 120.9 | 1.48 | 1.44 | 1.51 | 25 |
| 19.c | $\frac{T'}{T_\circ} = 0.4; \frac{T''}{T_\circ} = 3.2$ | 81 | 132.0 | 1.50 | 1.26 | 1.52 | 33 |

| | | FSS(A+B) | | | | | |
|---|---|---|---|---|---|---|---|
| Case | perturbation | formed at Time (hrs) | formed at r ($R_\circ$) | ave. $M_f$ | $M_s$ at 140 $R_\circ$ | $M_s$ at 180 $R_\circ$ | second perturbation starts at(hrs) |
| 19.a | $\frac{T'}{T_\circ} = 0.4; \frac{T''}{T_\circ} = 3.2$ | 49 | 93.5 | 2.23 | 2.15 | 2.24 | 15 |

| | | FSS(A) | | | | | |
|---|---|---|---|---|---|---|---|
| Case | perturbation | formed at Time (hrs) | formed at r ($R_\circ$) | ave. $M_f$ | $M_s$ at 140 $R_\circ$ | $M_s$ at 180 $R_\circ$ | second perturbation starts at(hrs) |
| 19.a | $\frac{T'}{T_\circ} = 0.4; \frac{T''}{T_\circ} = 3.2$ | 13 | 33.1 | 1.36 | 29 | 59.0 | 15 |
| 19.b | $\frac{T'}{T_\circ} = 0.4; \frac{T''}{T_\circ} = 3.2$ | 13 | 32.7 | 1.623 | 81 | 145.9 | 25 |
| 19.c | $\frac{T'}{T_\circ} = 0.4; \frac{T''}{T_\circ} = 3.2$ | 13 | 33.1 | 1.72 | 113 | 184.5 | 33 |

| | | FSS(B) | | | | | |
|---|---|---|---|---|---|---|---|
| Case | perturbation | formed at Time (hrs) | formed at r ($R_\circ$) | ave. $M_f$ | $M_s$ at 140 $R_\circ$ | $M_s$ at 180 $R_\circ$ | second perturbation starts at(hrs) |
| 19.b | $\frac{T'}{T_\circ} = 0.4; \frac{T''}{T_\circ} = 3.2$ | 29 | 35.3 | 1.80 | 69 | 114.8 | 25 |
| 19.c | $\frac{T'}{T_\circ} = 0.4; \frac{T''}{T_\circ} = 3.2$ | 37 | 35.1 | 1.69 | 113 | 184.5 | 33 |

Where (A) denotes the shock generated by the first perturbation; (B) denotes the shock generated by the second perturbation; (A+B) denotes the merged shock from two shocks which were generated by the first and second perturbations.

Table VIIIa. Summary Results of Type VI Perturbations; Second Perturbation Starts at t = 15 hrs.

| | | FSS(A+B) | | | | |
|---|---|---|---|---|---|---|
| Case | perturbation | formed Time (hrs) | formed r $(R_s)$ | ave. $M_s$ | $M_s$ at 60 $R_s$ | $M_s$ at 200 $R_s$ |
| 20.b | $\frac{\rho'}{\rho_o} = 0.4, \frac{v_r'}{v_{r_o}} = 0.4; \frac{\rho''}{\rho_o} = 5.0, \frac{v_r''}{v_{r_o}} = 1.6$ | 25 | 49.9 | 3.14 | 3.40 | 2.84 |
| 21.b | $\frac{v_r'}{v_{r_o}} = 0.4, \frac{T'}{T_o} = 0.4; \frac{\rho''}{\rho_o} = 5.0, \frac{v_r''}{v_{r_o}} = 1.6$ | 25 | 48.6 | 3.46 | 4.56 | 2.35 |
| 22.b | $\frac{v_r'}{v_{r_o}} = 0.4, \frac{T'}{T_o} = 0.4; \frac{v_r''}{v_{r_o}} = 1.6, \frac{T''}{T_o} = 5.0$ | 25 | 48.1 | 3.16 | 4.44 | 2.47 |
| | | FFS(B) | | | | |
| Case | perturbation | formed Time (hrs) | formed r $(R_s)$ | ave. $M_s$ | $M_s$ at 60 $R_s$ | $M_s$ at 200 $R_s$ |
| 20.b | $\frac{\rho'}{\rho_o} = 0.4, \frac{v_r'}{v_{r_o}} = 0.4; \frac{\rho''}{\rho_o} = 5.0, \frac{v_r''}{v_{r_o}} = 1.6$ | 25 | 52.9 | 1.89 | 1.22 | 2.21 |
| 21.b | $\frac{v_r'}{v_{r_o}} = 0.4, \frac{T'}{T_o} = 0.4; \frac{\rho''}{\rho_o} = 5.0, \frac{v_r''}{v_{r_o}} = 1.6$ | 25 | 51.4 | 1.89 | 1.22 | 2.26 |
| 22.b | $\frac{v_r'}{v_{r_o}} = 0.4, \frac{T'}{T_o} = 0.4; \frac{v_r''}{v_{r_o}} = 1.6, \frac{T''}{T_o} = 5.0$ | 25 | 51.5 | 1.96 | 1.16 | 2.02 |

Table VIIIb. Summary Results of Type VI Perturbation; Second Perturbation Starts at t = 33 hrs.

| | | FFS(B) | | | | |
|---|---|---|---|---|---|---|
| Case | perturbation | formed at Time (hrs) | formed at r ($R_*$) | ave. $M_s$ | $M_s$ at 60 $R_*$ | $M_s$ at 200 $R_*$ |
| 20.a | $\frac{\rho'}{\rho_o} = 0.4, \frac{v'_r}{v_{r_o}} = 0.4; \frac{\rho''}{\rho_o} = 5.0, \frac{v''_r}{v_{r_o}} = 1.6$ | 37 | 37.4 | 1.81 | 1.38 | 2.30 |
| 21.a | $\frac{v'_r}{v_{r_o}} = 0.4, \frac{T'}{T_o} = 0.4; \frac{\rho''}{\rho_o} = 5.0, \frac{v''_r}{v_{r_o}} = 1.6$ | 49 | 66.3 | 1.83 | 1.10 | 1.95 |
| 22.a | $\frac{v'_r}{v_{r_o}} = 0.4, \frac{T'}{T_o} = 0.4; \frac{v''_r}{v_{r_o}} = 1.6, \frac{T''}{T_o} = 5.0$ | 37 | 37.8 | 1.95 | 1.20 | 2.58 |

| | | FSS(B) | | | | |
|---|---|---|---|---|---|---|
| Case | perturbation | formed Time (hrs) | formed r ($R_*$) | ave. $M_s$ | disappeared Time (hrs) | disappeared r ($R_*$) |
| 20.a | $\frac{\rho'}{\rho_o} = 0.4, \frac{v'_r}{v_{r_o}} = 0.4; \frac{\rho''}{\rho_o} = 5.0, \frac{v''_r}{v_{r_o}} = 1.6$ | 41 | 45.23 | 1.97 | 85 | 147. |
| 21.a | $\frac{v'_r}{v_{r_o}} = 0.4, \frac{T'}{T_o} = 0.4; \frac{\rho''}{\rho_o} = 5.0, \frac{v''_r}{v_{r_o}} = 1.6$ | 37 | 35.86 | 1.45 | 73 | 116.8 |
| 22.a | $\frac{v'_r}{v_{r_o}} = 0.4, \frac{T'}{T_o} = 0.4; \frac{v''_r}{v_{r_o}} = 1.6, \frac{T''}{T_o} = 5.0$ | 37 | 36.33 | 1.53 | 73 | 119.2 |

| | | FSS(A) | | | | |
|---|---|---|---|---|---|---|
| Case | perturbation | formed Time (hrs) | formed r ($R_*$) | ave. $M_s$ | disappeared Time (hrs) | disappeared r ($R_*$) |
| 20.a | $\frac{\rho'}{\rho_o} = 0.4, \frac{v'_r}{v_{r_o}} = 0.4; \frac{\rho''}{\rho_o} = 5.0, \frac{v''_r}{v_{r_o}} = 1.6$ | 13 | 31.1 | 2.71 | 85 | 154.8 |
| 21.a | $\frac{v'_r}{v_{r_o}} = 0.4, \frac{T'}{T_o} = 0.4; \frac{\rho''}{\rho_o} = 5.0, \frac{v''_r}{v_{r_o}} = 1.6$ | 13 | 31.9 | 2.58 | 101 | 187.1 |
| 22.a | $\frac{v'_r}{v_{r_o}} = 0.4, \frac{T'}{T_o} = 0.4; \frac{v''_r}{v_{r_o}} = 1.6, \frac{T''}{T_o} = 5.0$ | 11 | 29.6 | 2.00 | 89 | 162. |

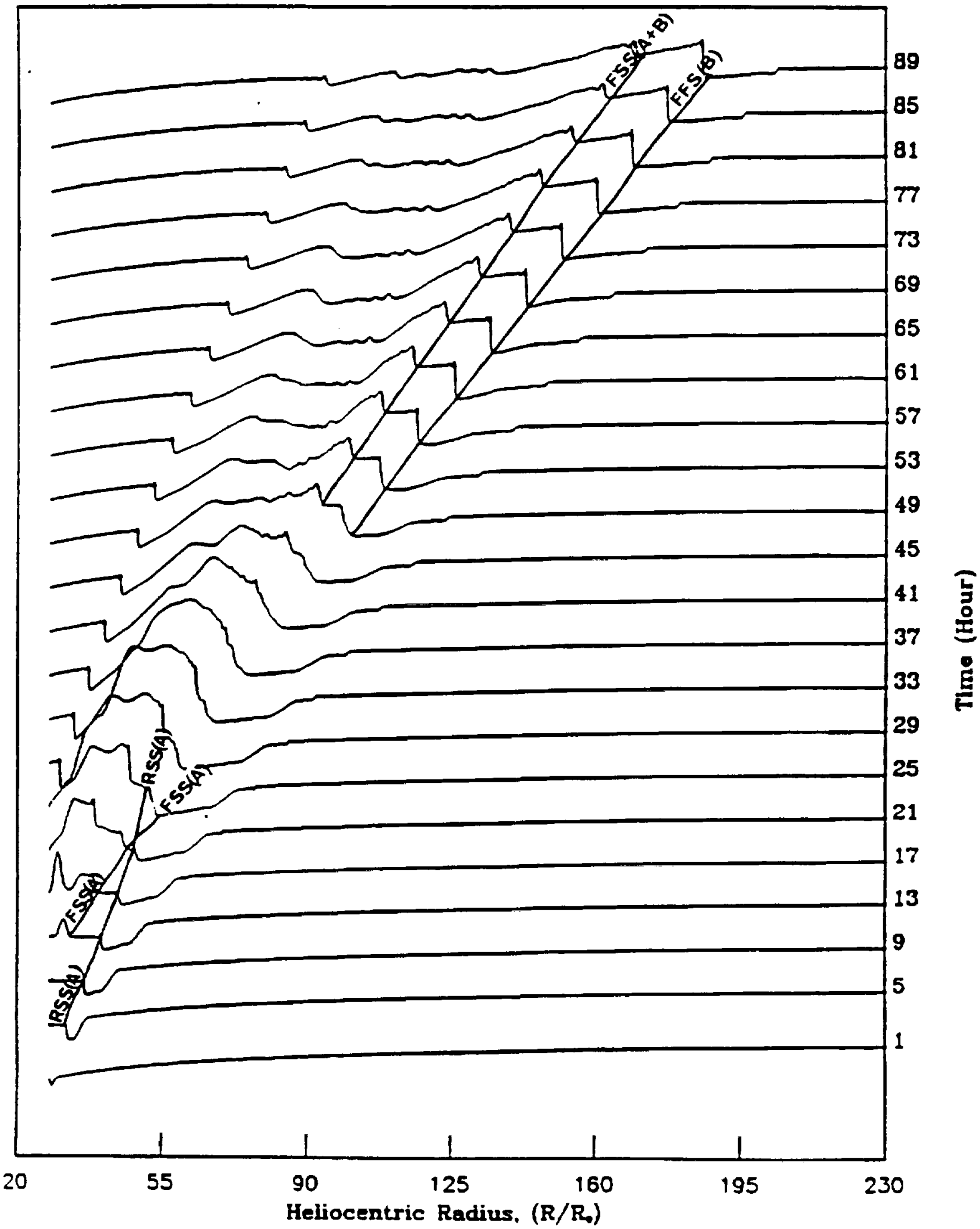


Figure 4. The evolution of radial velocity for case 19a, $\frac{\rho'}{\rho_O}=0.4$, $\frac{\rho''}{\rho_O}=3.2$

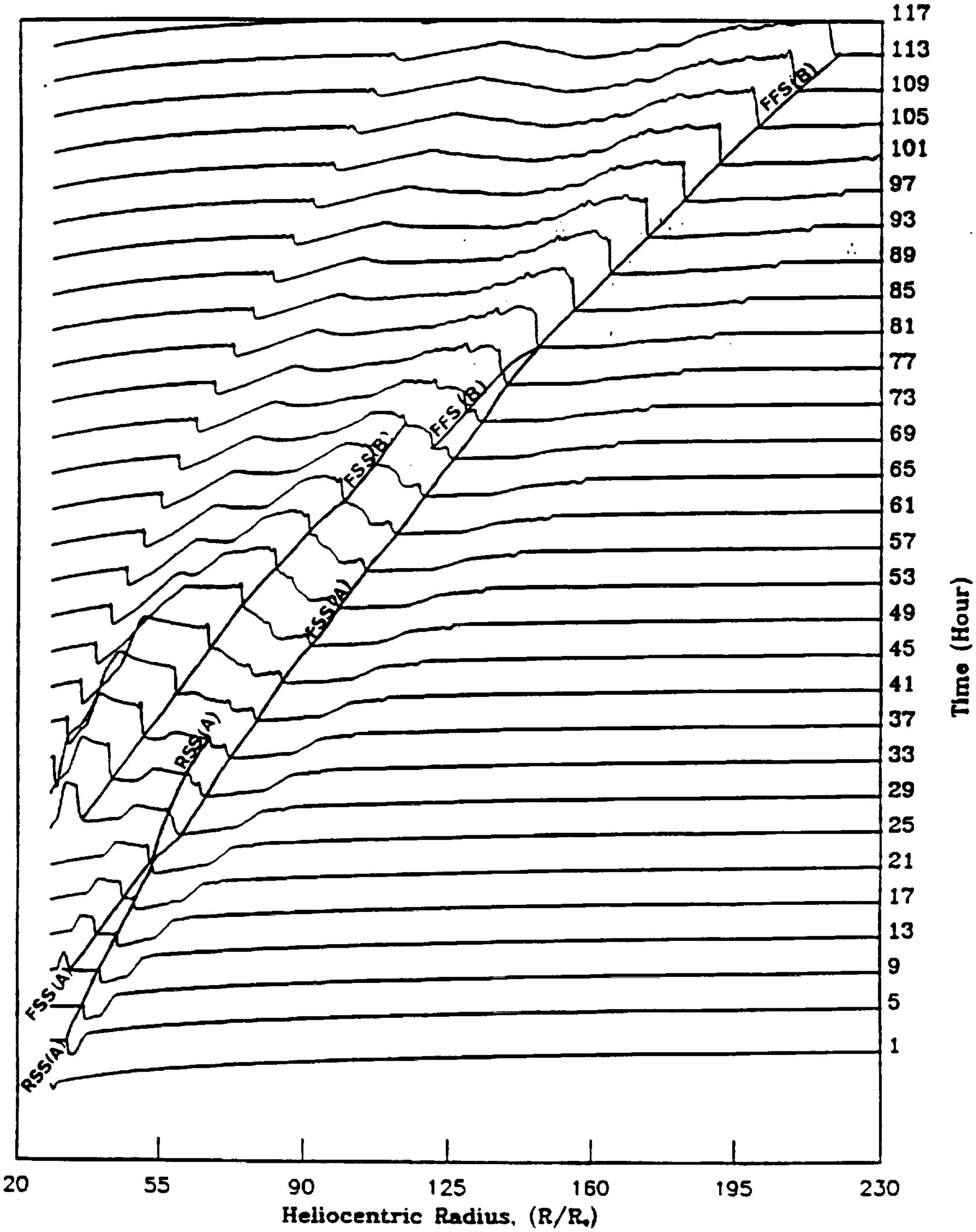


Figure 5. The evolution of radial velocity for case 19b, $\frac{\rho'}{\rho_0} = 0.4$, $\frac{\rho''}{\rho_0} = 3.2$

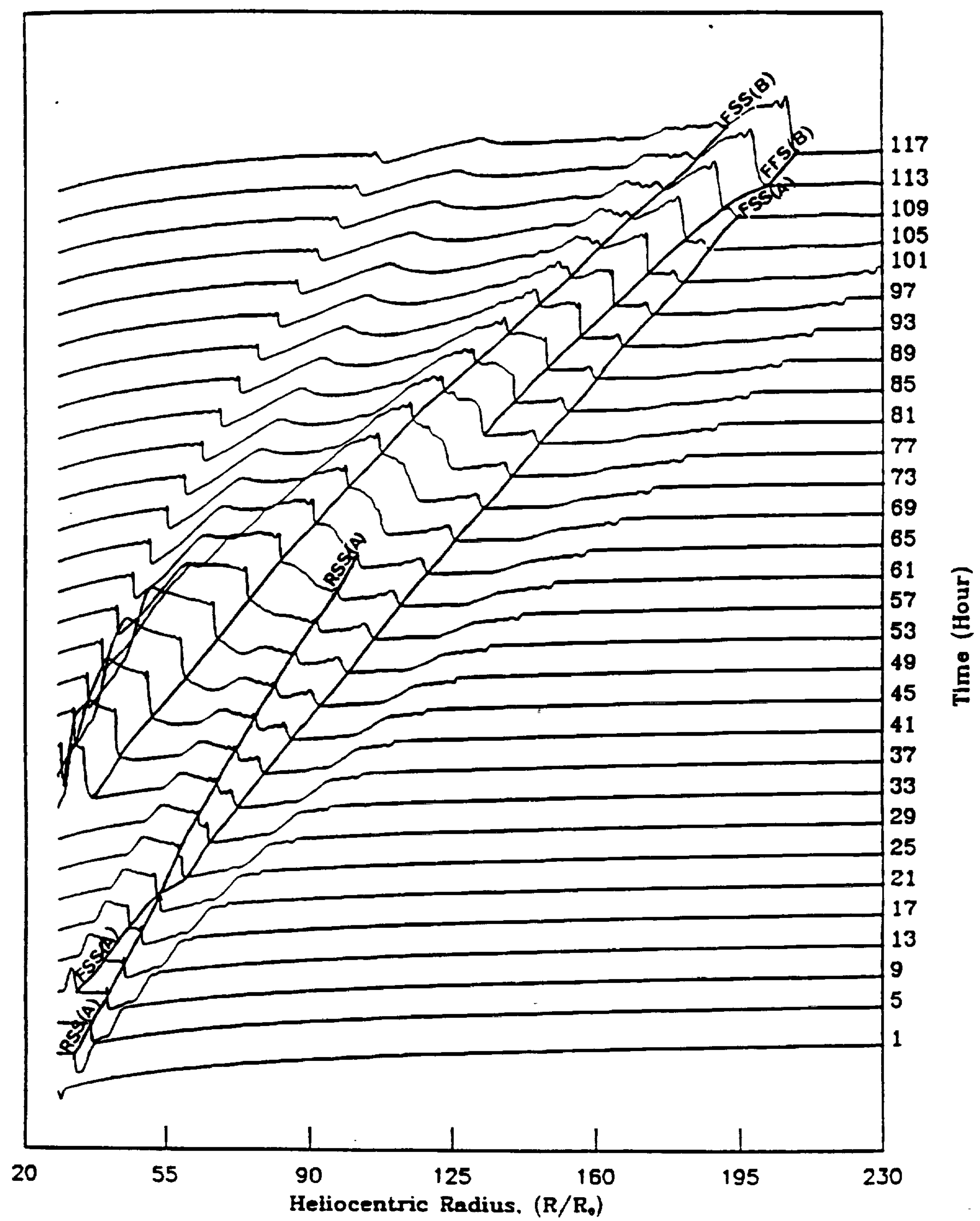


Figure 6. The evolution of radial velocity for case 19c, $\frac{\rho'}{\rho_O} = 0.4$, $\frac{\rho''}{\rho_O} = 3.2$

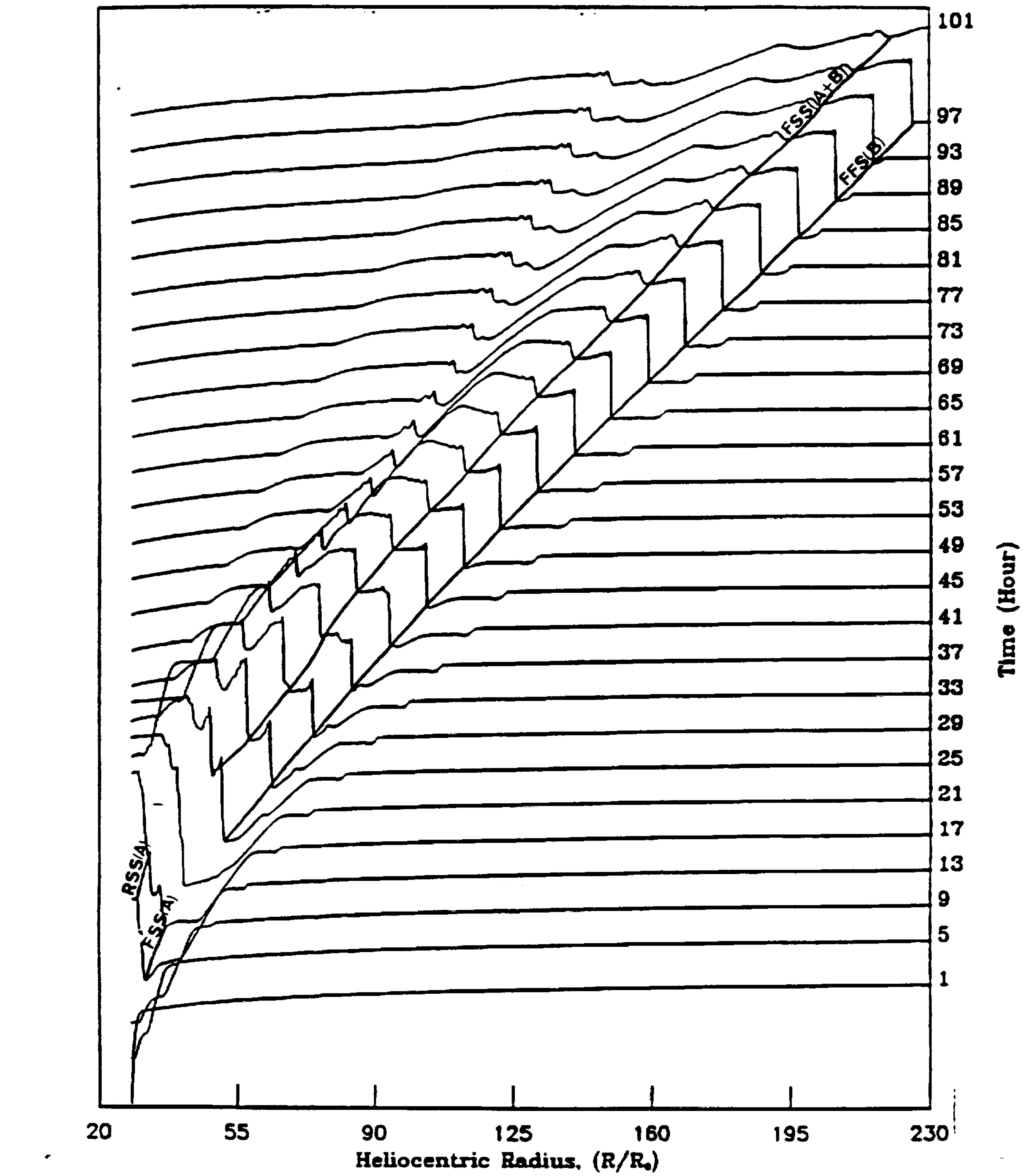


Figure 7. The evolution of radial velocity for case 21b, $\dfrac{v'}{v_{r_o}} = 0.4$, $\dfrac{T'}{T_o} = 0.4$; $\dfrac{\rho''}{\rho_o} = 5.0$, $\dfrac{v''_r}{v_{r_o}} = 1.6$.

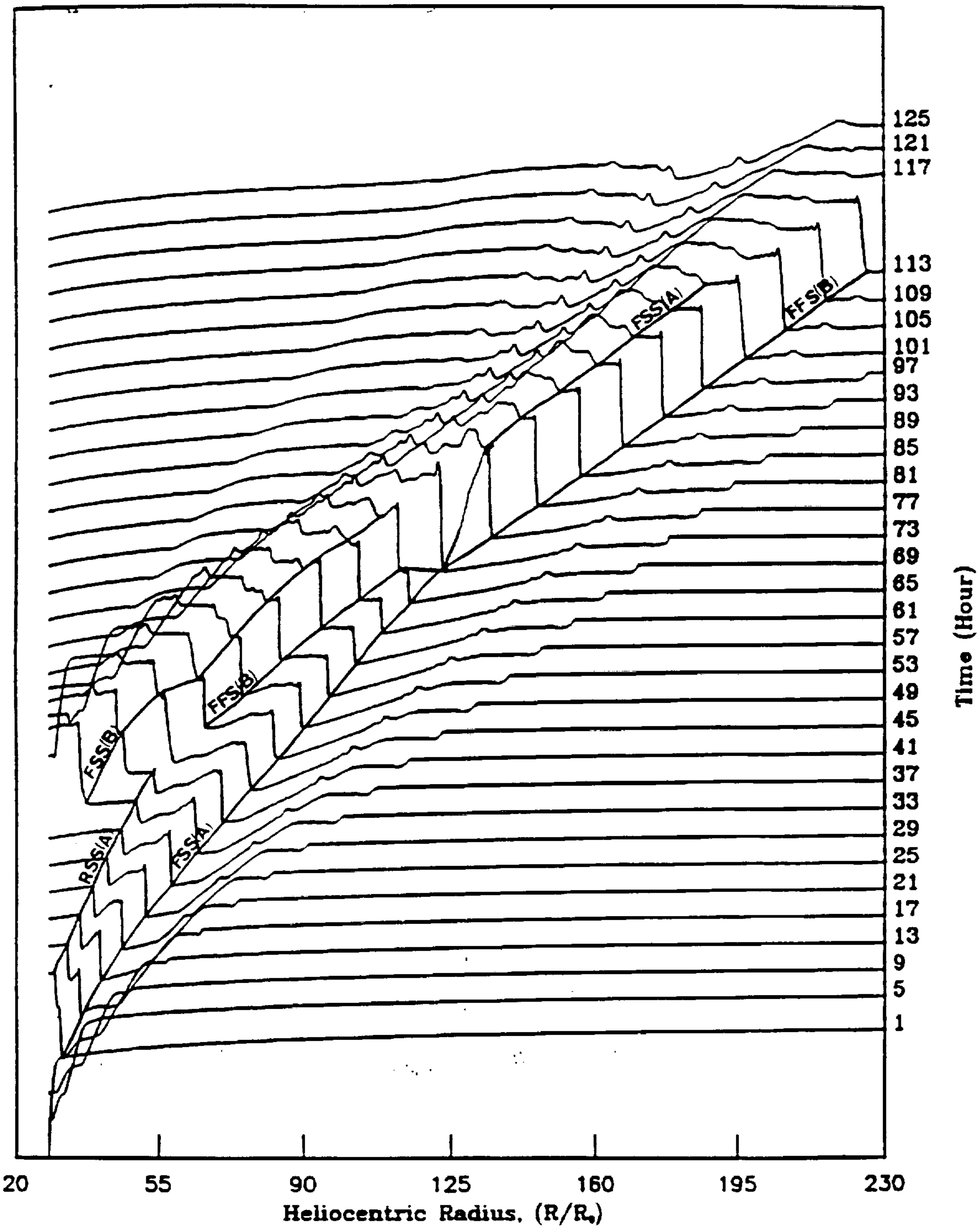


Figure 8. The evolution of radial velocity for case 21a, $\dfrac{v'}{v_{r_o}} = 0.4$, $\dfrac{T'}{T_o} = 0.4$; $\dfrac{\rho''}{\rho_o} = 5.0$, $\dfrac{v''_r}{v_{r_o}} = 1.6$.

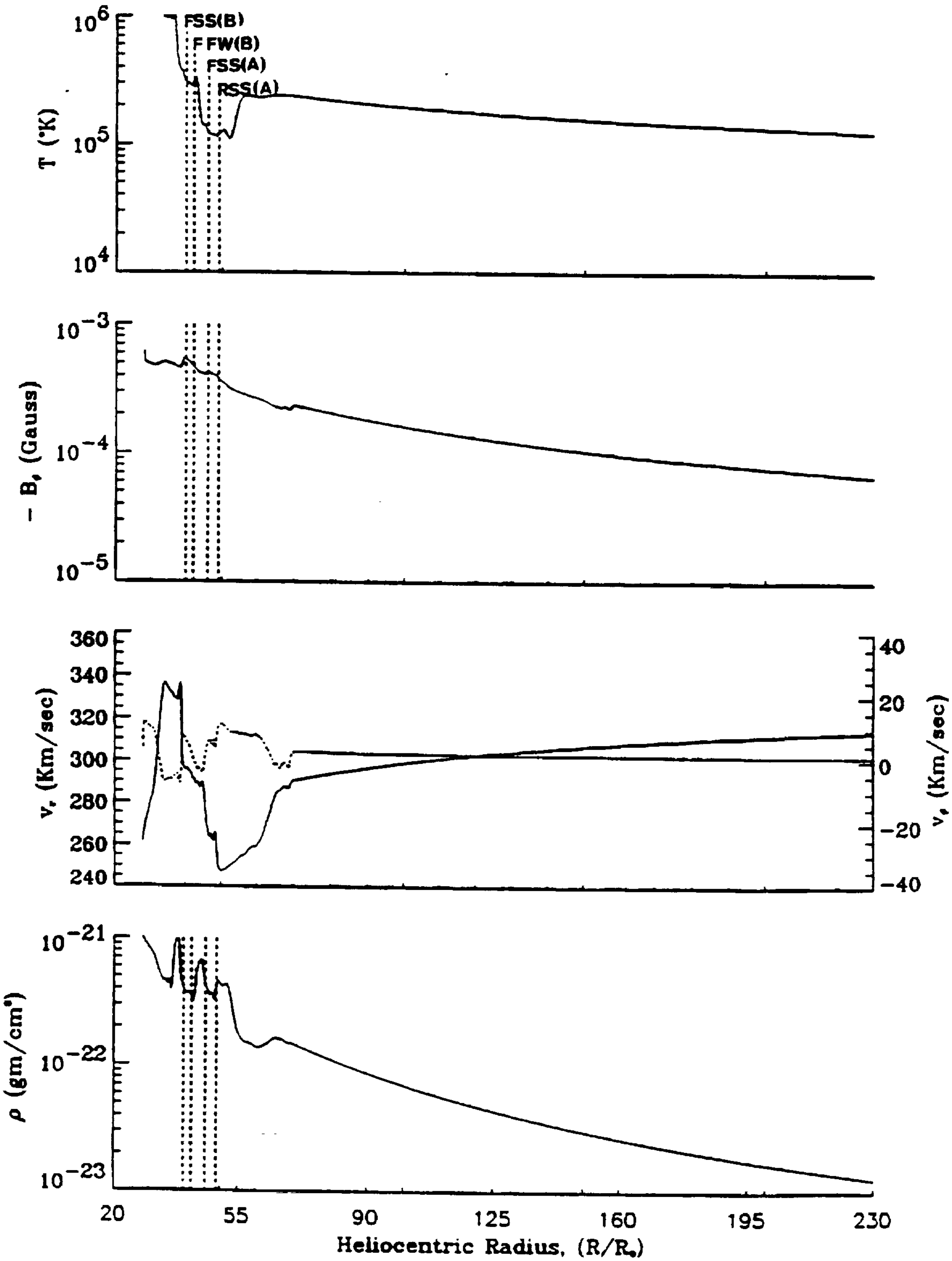


Figure 9. The solar solution versus heliocentric distance at t = 21 hrs of case 19a, $\frac{\rho'}{\rho_o} = 0.4$, $\frac{\rho''}{\rho_o} = 3.2$

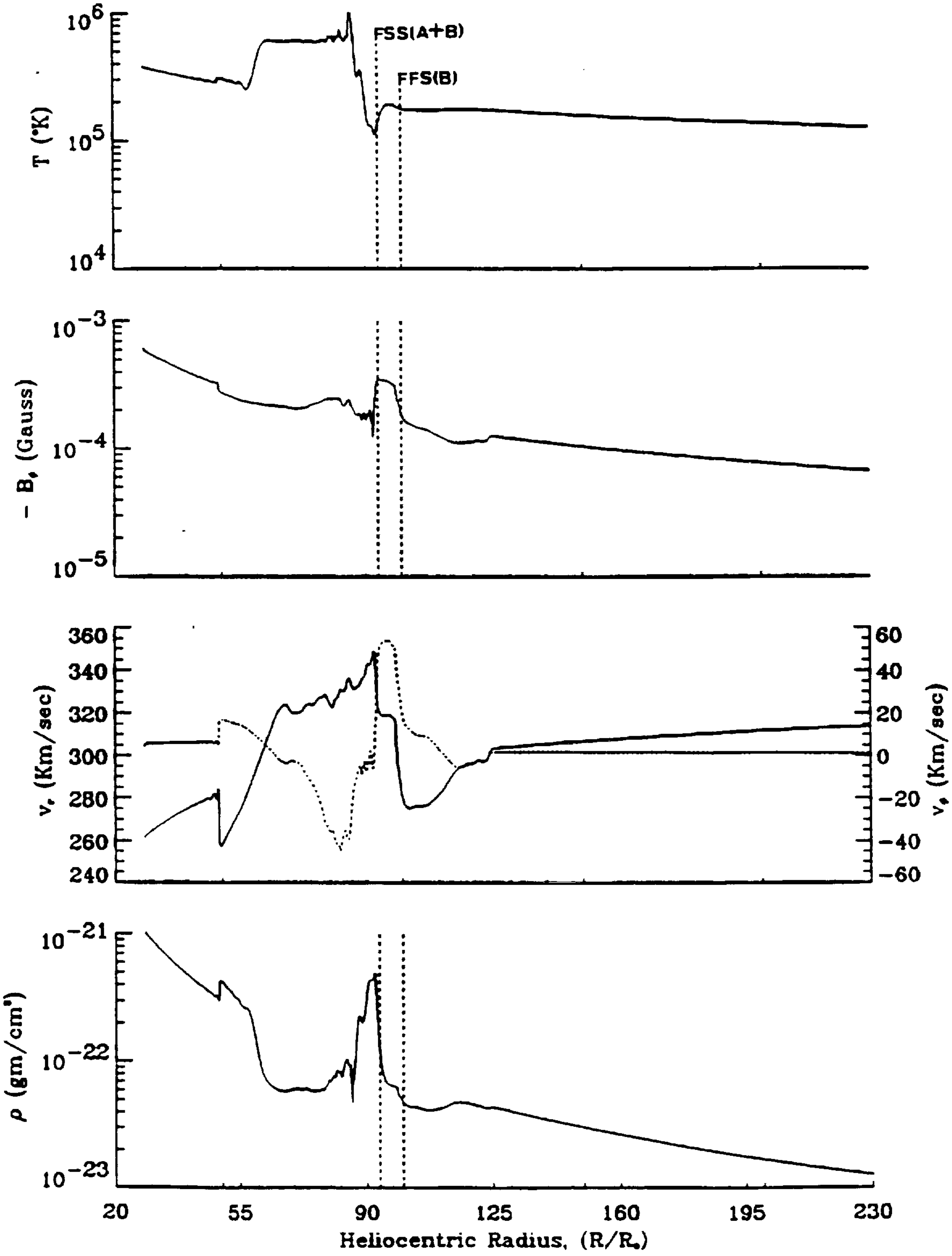


Figure 10. The solar solution versus heliocentric distance at t = 49 hrs of case 19a, $\frac{\rho'}{\rho_o} = 0.4$, $\frac{\rho''}{\rho_o} = 3.2$

## SUMARY

On the basis of these twenty-two numerical experiments, we found:

1. The forward slow shock (FSS) and reversed slow shock (RSS) can pass through each other and keep its own characteristics.
2. The second FSS will catch the first FSS and emerge into a stronger FSS.
3. The FSS always disappears within a distance of 140 $R_S$ (solar radii) from the sun when there is a forward fast shock propagating in front of them.
4. When a FSS propagates behind a forward fast shock (FFS), it shows decreasing mach number of FSS.
5. When a FSS propagates in front of a FFS, it always will be caught by the FFS and destroyed by it.
6. In all the tests we have performed we have not discovered that the FSS (RSS) evolves into a FFS.

This work is supported by NASA Headquarters Grant NAGW-9